

Contents list available at CBIORE journal website

International Journal of Renewable Energy Development

Journal homepage: https://ijred.cbiore.id



Research Article

Morphological and thermal stability analysis of Sn/C electrodes synthesized through impregnation and precipitation methods for CO₂ electroreduction

Mitra Eviani^{a,b} , Tirto Prakoso^a, Dadan Kusdiana^b, Pramujo Widiatmoko^a, Hary Devianto^a

Abstract. This study investigates tin (Sn) based electrodes supported by graphite for the electrochemical reduction of carbon dioxide (ECO₂R) to formic acid, comparing precipitation and impregnation synthesis methods. Electrodes were characterized using Scanning Electron Microscopy (SEM), Energy Dispersive Spectroscopy (EDS), Thermogravimetric Analysis (TGA), Cyclic Voltammetry (CV), Chronoamperometry, and Electrochemical Impedance Spectroscopy (EIS). The precipitation method yielded higher Sn content (91.22%) and superior thermal stability (3% mass loss at 1000°C vs. 45% for impregnation). Morphological analysis through SEM revealed precipitation-synthesized electrodes exhibited more uniform Sn particle distribution across the graphite surface, while impregnation resulted in larger Sn agglomerates with less homogeneous coverage, significantly influencing electroactive surface area and catalytic performance. The electrochemical performance of electrodes was tested using H-cell. CV showed decreased cathodic current for Sn/C electrodes compared to pure graphite in CO2-saturated electrolyte, while chronoamperometry indicated slightly better sustained performance for precipitation-synthesized electrodes with stabilized current densities after 3 hours of operation. EIS analysis suggested the precipitation method yields a marginally lower ohmic resistance (28.8 \, \Omega \, vs. 29.8 \, \Omega), resulting in a more favorable electrode structure for overall catalytic activity. Both methods showed lower ohmic resistance than that of pure graphite (38.1 Ω), the precipitation-synthesized Sn/C electrode emerged as the preferred selection for ECO₂R to formic acid, balancing high Sn content, thermal stability, superior durability, and better Faradaic efficiency. The observed performance differences were attributed to distinct metal-support interactions formed during synthesis, with precipitation creating stronger metal-carbon bonds that enhance stability but potentially limit certain active sites necessary for optimal CO2 reduction kinetics. This comprehensive characterization revealed that the precipitation-synthesized electrode offers the most promising foundation for further development, potentially through process optimization, hybrid synthesis approaches, or targeted doping strategies to enhance catalytic activity while maintaining the advantageous stability characteristics.

Keywords: Tin electrodes, CO₂ electroreduction, precipitation, impregnation, carbon support



@ The author(s). Published by CBIORE. This is an open access article under the CC BY-SA license (http://creativecommons.org/licenses/by-sa/4.0/).

Received: 9th Nov 2024; Revised: 16th May 2025; Accepted: 22th June 2025; Available online: 3rd July 2025

1. Introduction

The electrochemical reduction of carbon dioxide (CO_2), commonly known as ECO_2R , has attracted significant scientific and industrial interest as a leading strategy for mitigating greenhouse gas emissions and transitioning toward a circular carbon economy. With global CO_2 emissions reaching a record level of approximately 37.4 billion metric tons in 2023, the urgency to develop effective carbon capture and utilization (CCU) technologies has never been more pronounced (IEA, 2024). ECO_2R leverages renewable electricity to transform waste CO_2 into valuable chemicals and fuels, thereby contributing to the decarbonization of industrial processes and reducing dependency on fossil feedstocks ($Liu\ et\ al.$, 2023).

Among the various catalytic materials investigated for ECO_2R , metal-based electrodes, especially tin (Sn), have demonstrated exceptional efficiency and selectivity as catalysts for the ECO_2R reaction, primarily due to their capacity to

generate formic acid, with relatively low onset potentials and high Faradaic efficiencies while suppressing the hydrogen evolution reaction (HER) (Álvarez-Gómez & Varela, 2023; Lim et al., 2020; Monteiro et al., 2022; Ren et al., 2020; Yao et al., 2023).

Formic acid represents a particularly valuable target product due to its applications as a hydrogen carrier, preservative, and chemical intermediate. The global formic acid market is expected to grow significantly, with a projected value exceeding USD 3.13 billion by 2032 (Maximize Market Research, 2024). Recent studies have shown that Sn electrodes can achieve Faradaic efficiencies for formic acid production exceeding 80% under optimized conditions (Bashir *et al.*, 2016; del Castillo *et al.*, 2015; Kim *et al.*, 2014; Q. Li *et al.*, 2017; Wen *et al.*, 2018; Won *et al.*, 2015; Wu *et al.*, 2021; Yang *et al.*, 2020; R. Zhang, Lv, Li, & Lei, 2015; R. Zhang, Lv, Li, Mezaal, *et al.*, 2015; C. Zhao *et al.*, 2016; Q. Zhu *et al.*, 2016).

^aDepartment of Chemical Engineering, Bandung Institute of Technology, Ganesha no. 10, Bandung, West Java, 40132, Indonesia

^bCenter for Oil and Gas Testing, Ministry of Energy and Mineral Resources, Ciledug Raya Kav. 109, South Jakarta, 12230, Indonesia

^{*} Corresponding author(s)
Email: hardev@itb.ac.id (H. Devianto)

Despite these promising results, several critical challenges continue to impede the commercial viability of Sn-based ECO₂R systems. A significant difficulty in the advancement of Sn-based catalysts is improving their durability and catalytic efficiency during the electrochemical process. Sn electrodes often suffer from rapid deactivation due to surface poisoning, agglomeration, and detachment during extended operation. Additionally, mass transport limitations, competing hydrogen evolution reactions, and insufficient CO₂ solubility in aqueous electrolytes further compromise performance (Álvarez-Gómez & Varela, 2023; Varhade *et al.*, 2025; S. Zhao *et al.*, 2019).

To address these challenges, researchers have explored various strategies for enhancing Sn catalyst performance. To enhance stability and catalytic activity, pure metal catalysts are combined with additional elements to generate novel catalysts exhibiting improved performance. The modification of electrode surfaces through alloying, oxidation state control, nano-structuring, and support optimization has shown considerable promise. The utilization of diverse integrated electrodes (such as metals, metal oxides, and metal alloys/intermetallic), along with the integration of promoters and/or carbon supports, with or without nitrogen doping, is anticipated to significantly enhance the performance of CO2 electrochemical reduction. Recent studies have demonstrated that bimetallic Sn-based catalysts (e.g., Cu-Sn, Ag-Sn) can achieve improved selectivity and reduced overpotentials compared to monometallic systems (Bashir et al., 2016; Ren et al., 2020; Wang et al., 2019; Widiatmoko et al., 2020).

Carbon support materials, particularly graphite, demonstrate significant potential as essential components in electrocatalyst systems. Graphite's substantial surface area facilitates homogeneous distribution of Sn catalysts, increasing the number of active catalytic sites and enhancing reaction efficiency. Its porous structure optimizes mass and electron transport, accelerating overall reaction rates, while the characteristic lamellar arrangement enables rapid electron mobility critical for electrochemical processes (Yu et al., 2023). Beyond these advantages, graphite exhibits superior electrical conductivity, thermal stability, and chemical resistanceproperties that collectively extend electrode longevity (Safaei et al., 2018; Satola et al., 2016). Unlike alternative carbon materials such as carbon nanotubes or graphene oxide, graphite offers distinct advantages for ECO2R applications through its costeffectiveness, scalability, and well-established industrial production methods. These practical benefits, combined with exceptional physicochemical properties, position graphite as a particularly valuable support material for advancing electrocatalyst performance and durability in sustainable energy conversion technologies.

Despite the growing body of research on carbon-supported Sn catalysts, several critical knowledge gaps remain. First, direct comparisons between different synthesis methods for Sn/C electrodes are limited, making it difficult to identify optimal preparation techniques. Second, systematic studies correlating the physicochemical properties of Sn/C electrodes with their electrochemical performance for CO₂ reduction are scarce. Finally, understanding of how carbon supports influence the catalytic activity of Sn for formic acid production is still evolving.

This study addresses these knowledge gaps by investigating the modification of Sn electrodes supported by graphite through two distinct synthesis methods: precipitation and impregnation. While previous research has explored these methods independently for catalyst preparation, their comparative effectiveness specifically for Sn/C electrodes in ECO $_2\mathrm{R}$ applications has not been systematically evaluated. The precipitation approach facilitates the creation of homogeneous

Sn particles on the carbon surface, leading to a consistent distribution of catalytic active sites (Q. Wang et al., 2017). The impregnation process is utilized to incorporate Sn into the pores and surface of graphite, enhancing the interaction between the catalyst and the reactants, while optimizing electron transfer (Ali et al., 2022). This research focused on a comprehensive comparative analysis of precipitation versus impregnation methods for Sn/C electrode preparation specifically targeted for ECO2R to formic acid as well as detailed characterization of the structural, thermal, and electrochemical properties of these establish structure-property-performance electrodes to relationships (Shaikh et al., 2023). By explaining both aspects, this study aims to develop electrodes with enhanced catalytic performance and stability by utilizing various modification techniques and maximizing the benefits of graphite as a support, thereby advancing material effectiveness and electrolysis cell design for ECO2R technology. The findings are expected to contribute significantly to the ongoing efforts to develop economically viable and environmentally sustainable ECO2R systems for industrial implementation.

2. Material and method

The enhancement of ECO_2R can be achieved by selecting and modifying electrode structures. The cathode selection process encompasses multiple phases, starting with the synthesis of tin (Sn) and graphite. The methods employed for the manufacture or modification of the electrocatalyst comprise precipitation and impregnation procedures. The second stage comprises the production of electrodes utilizing electrocatalysts synthesized through precipitation and impregnation techniques, which are applied to carbon paper using spray and drop coating methods

2.1 Catalyst Synthesis Procedures

2.1.1 Precipitation Method

The precipitation process commences with the manufacture of activated carbon suspended in demineralized water (aqua DM), succeeded by the incremental addition of tin (II) chloride precursor solution (SnCl_{2.}2H₂O) in quantities of 0.9, 1.8, and 3.6 g. To elevate pH and facilitate precipitation, 0.8 g of NaOH is introduced, along with 10 mL of methanol (MeOH) to enhance the dispersion of the metal precursor on the activated carbon and expedite drying. The precipitation reagent is gradually introduced and agitated with a magnetic stirrer at ambient temperature to facilitate complete dissolution, yielding a precipitate of Sn particles. The precipitate is subjected to filtration, washing, and drying in a vacuum oven at 50°C for 4 hours, thereafter, undergoing heat treatment in a muffle furnace at 550°C to eliminate residual chemicals and impurities. The resulting electrocatalyst powder is subjected to calcination at a designated temperature to improve its crystallinity and stability.

2.1.2 Impregnation Method

The manufacture of the electrocatalyst using the impregnation method employs the identical precursor ($SnCl_2 \cdot 2H_2O$ solution) in differing quantities of 1, 2, and 3 g. Hydrochloric acid is introduced to solubilize the metal precursor, resulting in a homogenous solution. This enables the impregnation process, wherein the metal solution readily interacts with the graphite through a wet impregnation technique. The graphite is submerged in the solution until its entire surface is saturated with the metal solution. After impregnation, the mixture is agitated once more for uniformity, followed by drying in a vacuum oven at $70^{\circ}C$ to remove the

solvent and produce uniformly dispersed metal salts on the surface of the support material. The concluding phase involves calcination at an elevated temperature of 550°C to transform the metal salts into metal oxides and enhance adhesion between the metal and the substrate.

2.2 Electrode Fabrication

The subsequent phase entails the production of Sn/C electrodes utilizing the electrocatalyst powder produced via precipitation and impregnation techniques, which is applied to carbon paper through two methods: spray coating and drip coating. Spray coating is a method in which a solution containing the electrocatalyst is applied to the substrate surface, facilitating uniform dispersion of the catalyst material over the electrode surface. Conversely, drip coating entails the gradual application of the electrocatalyst solution over the substrate surface, facilitating adherence and resulting in a thicker layer than that achieved with spray coating. The electrocatalyst ink is formulated by dispersing 3 mg/cm² of electrocatalyst powder in a solution of 100 mg of Nafion (5 wt%) and 1.2 mL of isopropyl alcohol (99.7 wt%).

2.3 Characterization Techniques

2.3.1 Physical Characterization

The performance and durability of the modified Sn/C electrodes are subsequently evaluated using material characterization techniques, such as Scanning Electron Microscopy (SEM), Energy Dispersive Spectroscopy (EDS), and Thermogravimetric Analysis (TGA). SEM analysis was employed to examine the surface morphology and particle distribution of the synthesized electrocatalysts. EDS measurements were conducted to determine the elemental composition and distribution of tin on the graphite support. TGA was performed to assess the thermal stability and decomposition characteristics of the prepared electrodes.

2.3.2 Electrochemical Characterization

This study utilizes a modified H-type cell reactor for ECO_2R , as shown in Fig.1. The designed reactor comprises three chambers: a CO_2 capture chamber, an anode chamber with Pt-Ir electrodes, and a cathode chamber with Sn/C electrodes, separated by a Nafion 212 membrane. The CO_2 capture chamber is equipped with a bubbler that generates micrometer-sized CO_2 bubbles (microbubbles). A $0.5~M~KHCO_3$ solution serves as the catholyte for capturing CO_2 gas, while $0.1~M~H_2SO_4$

functions as the analyte. Prior to electrolysis experiments, the catholyte was bubbled with CO_2 for 1 hour to ensure CO_2 saturation

The electrochemical experiments were systematically conducted using several modified electrodes. Electrolysis was carried out for 3 hours under controlled conditions, followed by comprehensive electrochemical characterization employing Cyclic Voltammetry (CV), chronoamperometry, Electrochemical Impedance Spectroscopy (EIS). measurements were conducted in both N2 and CO2-saturated electrolytes to evaluate the catalytic activity of the electrodes toward CO₂ reduction. Subsequently, chronoamperometry tests were performed to assess the stability and long-term performance of the electrodes under constant potential conditions. For detailed interfacial analysis, EIS measurements were utilized to investigate the electrode resistance, charge transfer kinetics, and interface properties of the fabricated electrodes. EIS data were recorded over a frequency range of 100 mHz to 100 kHz using a potentiostat in a two-electrode configuration. Nyquist plots were generated from the EIS data, representing the imaginary part of impedance (Z") against the real part (Z'). Finally, data were fitted using equivalent circuit models to extract ohmic resistance, charge transfer resistance, and interfacial properties, which are critical for understanding electrode performance.

3. Result and Discussion

3.1 Synthesis of Sn Electrocatalyst with Carbon Support

To evaluate the effectiveness of the precipitation method in synthesising Sn-based electrocatalysts, a correlation study was first conducted between the precursor mass and the resulting Sn deposit. Fig.2 illustrates this relationship, indicating that as the precursor mass increases, the deposited Sn mass also rises in the precipitation method. Specifically, the Sn deposit percentage increases from 71.8% at 1 g of precursor to 87.5% at 2.5 g and ultimately reaches 91.2% at 3.5 g (Miki *et al.*, 2019). However, the trend is nonlinear, particularly between 1.8–3.6 g of precursor mass, which complicates efforts to predict or optimise the process at larger scales.

The precipitation method employed in this study is a straightforward and scalable approach, based on combining metal precursors with a precipitating agent to form metal or metal oxide precipitates. Recent developments have shown that hydrophobic modifications of hydroxyl-rich Sn surfaces can significantly improve both stability and selectivity under acidic

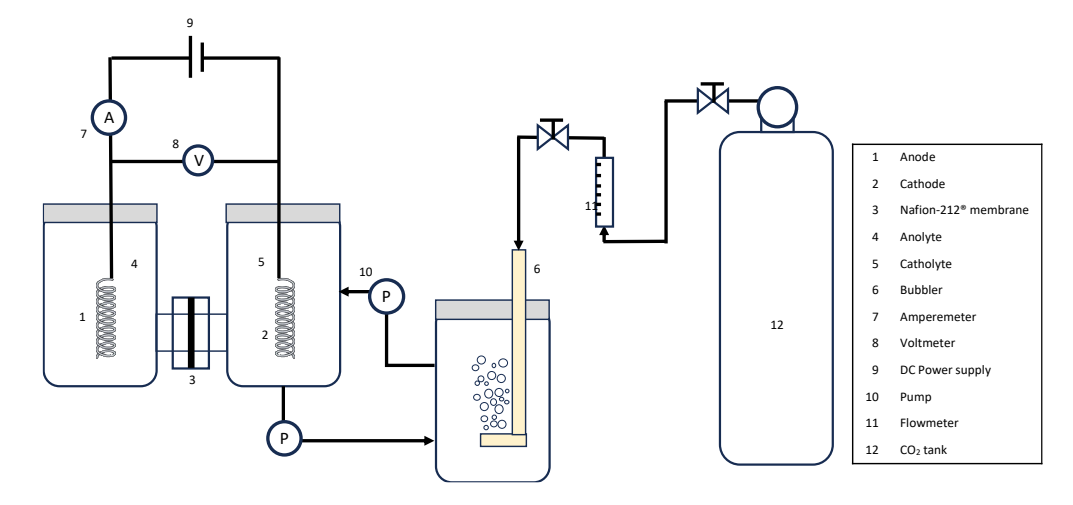


Fig 1. The experimental equipment diagram (H-cell)

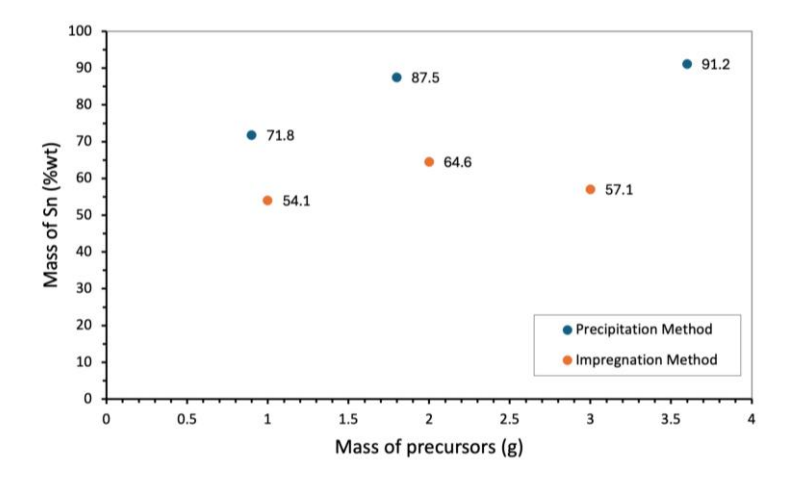


Fig 2. Comparison of Sn mass between precipitation and impregnation methods at various precursor masses

conditions, enabling over 95% Faradaic efficiency at high current densities (Y. Li *et al.*, 2025). By adjusting synthesis parameters such as pH and temperature, the process facilitates the formation of catalysts with consistent particle sizes and well-controlled morphologies (K. Zhang *et al.*, 2015). Moreover, the required equipment is relatively low-cost and easily accessible, making this technique particularly advantageous for industrial-scale production. Following this initial optimization and the successful synthesis of the electrocatalyst, physical characterization was carried out to assess the structural and morphological properties of the precipitated material. With these results confirming the suitability of the catalyst, the subsequent step involved depositing the material onto graphite sheets to fabricate functional electrodes.

To explore alternative strategies for incorporating Sn into composite electrodes, the impregnation method was evaluated. This approach allows the precursor solution to infiltrate the porous support material, enabling the formation of electrocatalysts directly within the electrode matrix. Fig.2 also illustrates the correlation between precursor mass and the resulting Sn content in the composite electrode using the impregnation method. As the precursor mass increases from 1 g to 3 g, the Sn content rises from 54.1 wt% to 64.6 wt%, suggesting that more precursor yields a higher loading until the support's capacity is approached. However, beyond 2 g of precursor, the mass of deposited Sn begins to diminish,

indicating a saturation effect that complicates further increases in Sn loading. This saturation suggests a limitation in Sn incorporation, likely due to surface interaction constraints and the porosity of the support material (K. Zhang *et al.*, 2015). When saturation sets in, the uneven distribution or potential agglomeration of Sn may lead to diminished overall catalytic efficiency of the electrode, as the exposure of the active sites becomes compromised.

Despite these challenges, the impregnation method remains widely employed in catalyst fabrication due to its superior control over the placement and distribution of active components. Nevertheless, scaling up the process presents additional difficulties. Maintaining consistent catalyst dispersion across larger electrode surfaces often requires more complex equipment and tighter process control, potentially increasing production costs. Therefore, while the method offers flexibility and precision at the laboratory scale, its scalability for industrial applications demands further optimisation.

3.2 Morphological Analysis

To investigate the morphology and elemental distribution of Sn-based electrodes with carbon support, scanning electron microscopy (SEM) and energy-dispersive X-ray spectroscopy (SEM-EDS mapping) analyses were performed on samples synthesised using two different methods: precipitation and impregnation. Recent studies using chemical foaming on carbon

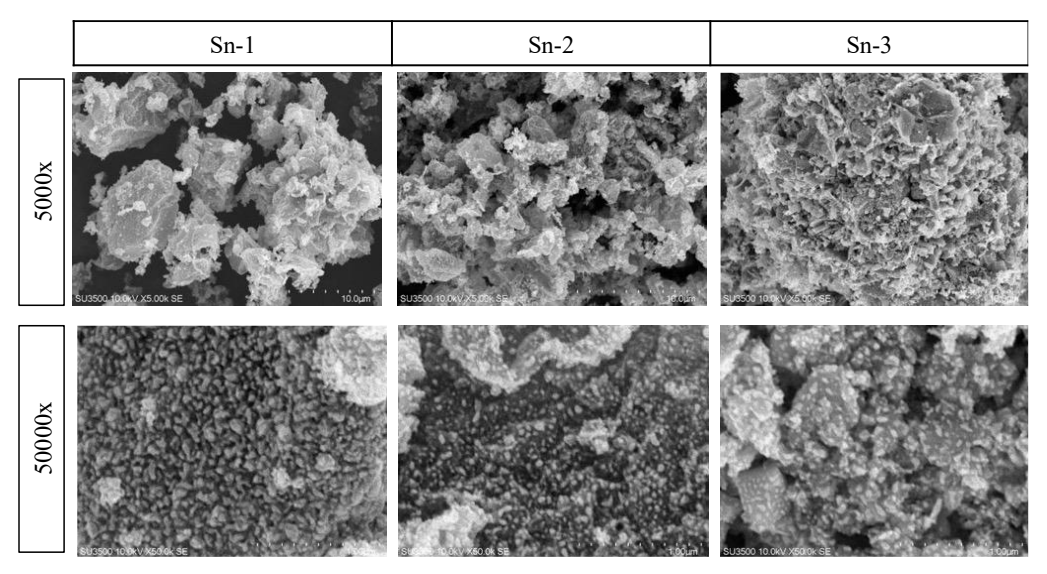


Fig 3. SEM characterization results of Sn/C electrodes using the precipitation method.

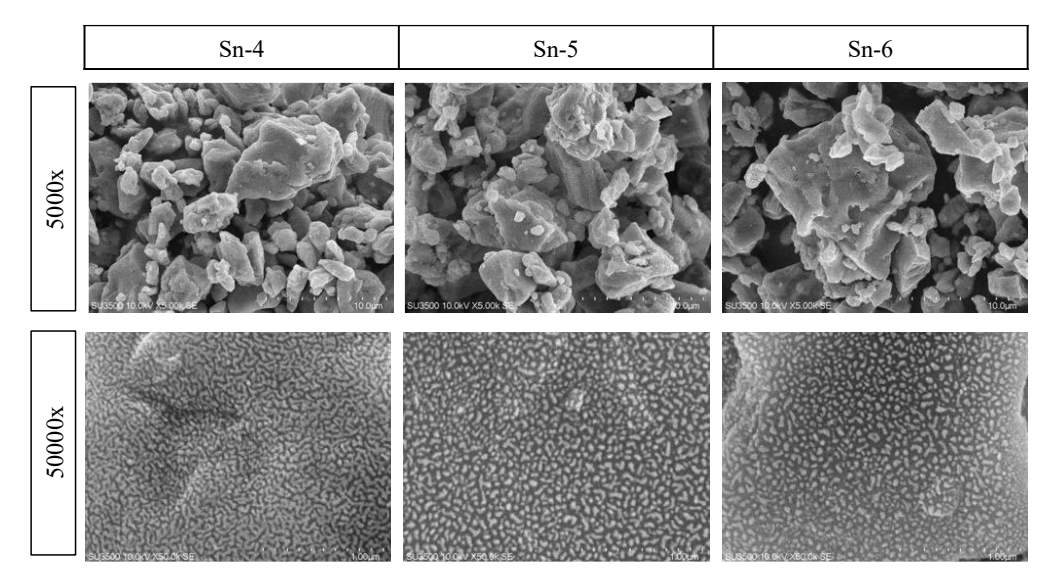


Fig 4. SEM characterization results of Sn/C electrodes using the impregnation method.

cloth supports have shown improved uniformity of Sn nanoparticle distribution, enhanced the electrochemical surface area and reduced agglomeration (C. Zhu *et al.*, 2025). The SEM results for the Sn/C electrodes corresponding to each method are presented in Fig.3 and Fig.4.

Fig.3 and Fig.4 show white granules visible on the graphite electrodes deposited with Sn, indicating that Sn was successfully deposited on the carbon surface. For electrodes prepared using the precipitation method, SEM analysis at 5,000x magnification shows that Sn is unevenly distributed and does not fully cover the graphite pores. However, at higher magnification (50,000×), Sn appears to be more uniformly distributed across the graphite surface. The more precursor added in this method, the more Sn adhered to the graphite surface. The amount of Sn adhering to the surface increases with higher precursor concentrations, and distinct changes in Sn grain size and morphology are observed as the precursor mass increases. In contrast, the impregnation method exhibits limited variation in Sn distribution despite increasing the precursor amount. This is particularly evident in samples Sn-5 and Sn-6, which show comparable Sn coverage, suggesting a saturation effect and restricted infiltration of the precursor into the graphite structure. The overall Sn deposition is less responsive to precursor variation compared to the precipitation method. These findings highlight that the precipitation method allows for greater tunability in Sn loading through precursor adjustment. Conversely, the impregnation method offers more consistent morphology but is less effective in increasing Sn content with additional precursor (Qu et al., 2023).

In addition to SEM analysis, EDS analysis along with Elemental Mapping was conducted to determine the elemental composition percentages and their distribution on the electrode

surface. Fig.5 shows the SEM-EDS mapping results for various electrode variations. Based on the SEM-EDS mapping data, it is evident that the amount and uniformity of Sn deposits on the graphite electrode surface increase as more precursor is added. The SEM-EDS mapping results indicate that Sn deposits on the graphite electrode surface became more abundant and evenly distributed with increasing SnCl₂·2H₂O precursor concentration, with the highest Sn content reaching 91.22%, as shown in Table 1. The effectiveness of the precipitation method in maximizing Sn content on the electrode can be attributed to the relationship between precursor concentration and the formation of SnO₂. Increasing the precursor amount directly correlates with a higher concentration of SnO2, which subsequently raises the Sn concentration on the carbon surface, as also displayed in Table 1. The presence of oxide or oxygen groups formed on the Sn/C electrodes is beneficial, as it enhances the hydrophilic properties, improving the performance of active sites on the electrode surface and facilitating chemical reactions (W. Li et al.,

This phenomenon is supported by various studies highlighting the importance of precursor composition in determining the structure and composition of the synthesized electrocatalyst. Botchway *et al.* (2023) reported that increasing Sn content in the precursor led to significant changes in the structure and morphology of Sn-based films and stressed the importance of precursor concentration in achieving desired material characteristics (Botchway *et al.*, 2023). In addition to influencing the structure and morphology of the electrocatalyst, varying the Sn concentration in the metal precursor also affects the optical and electrical properties of Sn-based thin films, demonstrating a direct impact of precursor concentration on material performance (Nkrumah *et al.*, 2023). Therefore, the

Table 1Elemental and oxide mass percentages from SEM-EDS Mapping of Sn/C electrodes using the precipitation method

Electrode _	Mass of Element (%wt)			Mass of Oxide Element (%wt)	
	С	Sn	0	С	SnO ₂
Sn-1	16.34	71.82	11.11	18.53	81.47
Sn-2	3.26	87.48	8.24	3.59	96.41
Sn-3	1.43	91.22	5.52	1.54	98.46

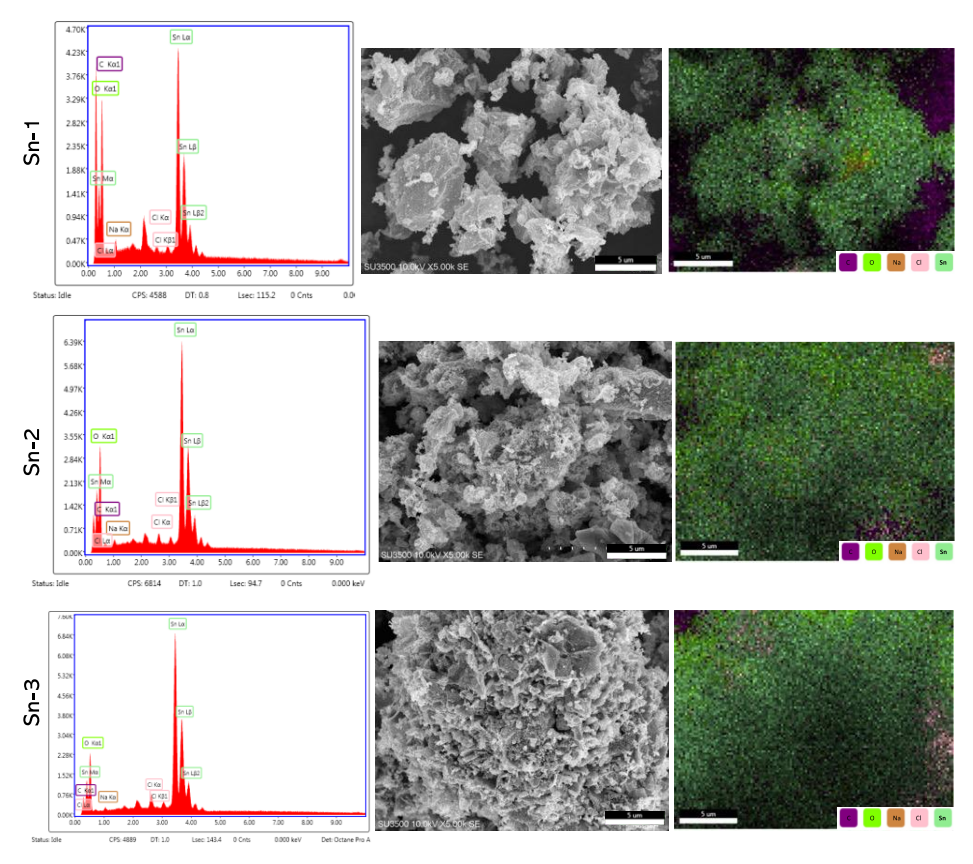


Fig 5. SEM-EDS Mapping results of Sn/C electrodes using the precipitation method.

Table 2Elemental and oxide mass percentages from SEM-EDS Mapping of Sn/C electrodes using the impregnation method

Electrode _	Mass of Element (%wt)			Mass of Oxide Element (%wt)	
	С	Sn	0	С	SnO ₂
Sn-4	29.17	54.08	9.54	35.04	64.96
Sn-5	20.93	64.59	5.66	24.47	75.53
Sn-6	26.08	57.09	5.68	31.36	68.64

ability of the precipitation method to maximize Sn content on the electrode is strongly supported by increasing precursor amounts, which play a crucial role in forming more SnO₂, subsequently boosting Sn concentration on the carbon surface and enhancing system performance.

The SEM-EDS Mapping results show that increasing the precursor amount also increases Sn percentage for the impregnation method, with the highest Sn content reaching 64.59% Sn and 75.53% SnO2 in sample Sn-5, as shown in Table 2. SEM-EDS mapping results for various electrode variations are displayed in Fig.6. Adding more than 2 grams of precursor in sample Sn-6 does not significantly increase the Sn percentage, indicating the occurrence of saturation. This saturation can be attributed to two factors. The first is the limited number of active sites on the carbon surface available to interact with Sn, so further Sn addition does not increase activity due to the lack of additional interaction sites (Del Castillo et al., 2014, 2017). The second factor could be due to limited precursor diffusion into the inner layers of the carbon structure, reducing the efficiency of impregnation at higher levels. Studies show that the morphology and porosity of carbon materials play a key role in determining how effectively the precursor can be distributed

throughout the structure (W. Li et al., 2016; H. Zhang et al., 2020).

Subsequent analysis of Sn grain size was conducted on the SEM images using the ImageJ software. High-resolution SEM images with sufficient magnification were imported into ImageJ, where the image scale was calibrated based on the scale bar provided. Grain size measurements were performed on multiple particles to ensure statistical representativeness, followed by statistical analysis to determine the average, median, and standard deviation of the particle sizes. The grain size data for Sn on various electrodes are summarised in Table 3.

Based on the SEM image analysis using ImageJ, Table 3 reveals interesting patterns in the Sn grain size distribution across the six different electrodes. While all electrodes consistently show a minimum grain size of 4 nm, there is a notable variation in the maximum grain size values. Electrodes Sn-1 through Sn-3 exhibit relatively smaller maximum grain sizes ranging from 13 to 27 nm. A significant increase in maximum grain size can be observed in electrodes Sn-4 through Sn-6, where the values jump dramatically to 112-121 nm. Specifically, both Sn-4 and Sn-5 show identical maximum grain sizes of 112 nm, while Sn-6 presents the largest grains at 121 nm. This substantial difference in maximum grain size between

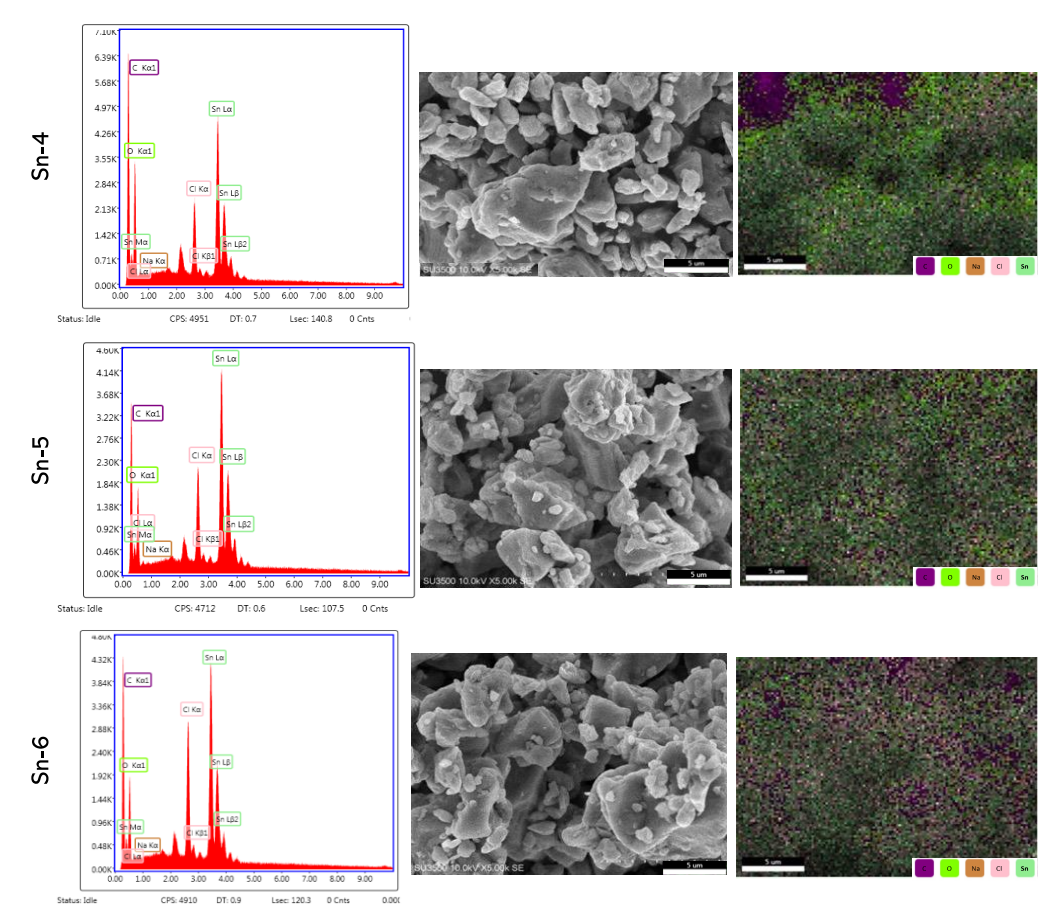


Fig 6. SEM-EDS Mapping results of Sn/C electrodes using the impregnation method.

Table 3The grain size for Sn on various electrodes

Sn grain size (nm)			
min	max		
4	13		
4	26		
4	27		
4	112		
4	112		
4	121		
	min 4 4 4 4 4		

the electrodes synthesized using the precipitation method (Sn-1 to Sn-3) and the electrodes synthesized using the impregnation method (Sn-4 to Sn-6) suggests distinct differences in the processing conditions or composition that influence grain growth during the electrode preparation.

The consistent minimum size of 4 nm across all electrodes indicates a similar nucleation process, while the varied maximum sizes point to different grain growth kinetics. These differences in grain size distribution are likely to influence the electrocatalytic performance of these Sn electrodes in CO2 electrolysis, particularly affecting parameters such as active surface area, electron transfer rates, and selectivity for specific carbon products. The electrodes with finer grain structure may provide more active sites for CO2 reduction, potentially enhancing catalytic activity and product selectivity, while those with larger grains might offer different stability characteristics during prolonged electrolysis operations. Further

electrochemical characterization would be necessary to correlate these microstructural features with the functional performance in CO_2 electroreduction applications.

Furthermore, the ImageJ analysis results were visualised using Kernel density distribution plots, as shown in Fig.7. This figure presents the Kernel density distributions of Sn grain sizes (in nm) for Sn-1 to Sn-6 electrodes. The horizontal axis (X) represents grain size, while the vertical axis (Y) corresponds to the Kernel density, providing an estimate of the size distribution within each dataset. The plot includes a legend indicating the corresponding colours and weight values (w) for each electrode.

The grain size distribution for electrode Sn-1 displays a sharp peak around 5 nm, indicating that most of the Sn grains are concentrated at this size. Electrodes Sn-2 and Sn-3 exhibit similarly located peaks, although with slightly lower densities, suggesting that Sn-1, Sn-2, and Sn-3 have relatively narrow and consistent size distributions despite increased precursor concentrations. In contrast, electrodes Sn-4, Sn-5, and Sn-6 exhibit broader distributions with multiple peaks in the range of 30-40 nm, reflecting greater variation in grain sizes. These results align with the SEM-EDS mapping data, which indicate that the precipitation method yields higher Sn content and a more homogeneous distribution. The weight values shown in the legend represent each electrode's contribution to the overall distribution, where Sn-1, despite having the highest density peak, contributes the least, whereas Sn-6, with the broadest distribution, contributes the most. The small vertical ticks along the bottom of the plot represent individual data points for each electrode variation, offering a visual indication of the variability and spread in grain size across the samples.

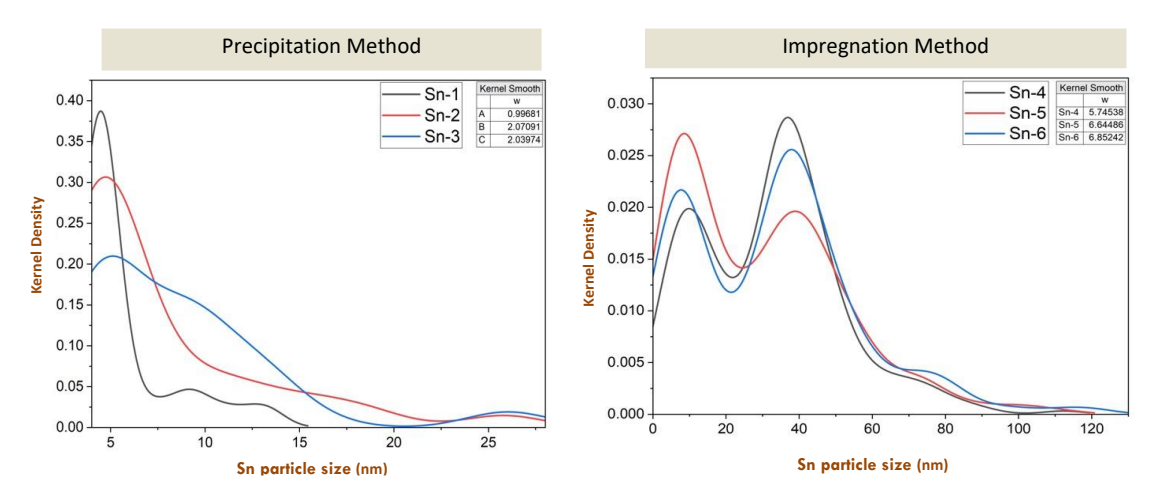


Fig 7. Kernel distribution graph for various electrodes

3.3 Thermal Stability Analysis

The graph in Fig.8 shows the TGA analysis results for the two synthesis methods used to produce electrocatalysts for electrochemical CO₂ reduction, namely the precipitation and impregnation methods. The precipitation and impregnation methods show significant differences in the thermal stability of the resulting electrocatalysts. For the precipitation method, the electrocatalyst exhibits excellent thermal stability. There is a relatively small mass loss in the temperature range of 0-1000°C, with a total mass loss of around 3% (H. Liu *et al.*, 2023). This indicates that the electrode synthesized via precipitation has a very stable structure, resistant to thermal degradation (Dinh *et al.*, 2018). The minimal mass loss is likely due to the evaporation of absorbed water or minor decomposition of organic components.

The precipitation method typically results in Sn particles being more strongly bound to the graphite surface through direct chemical reactions. The Sn particles formed are already in a more stable state and tend to remain on the graphite surface. As a result, less residue remains after the drying and calcination processes, leading to a lower mass loss during TGA. Calcination does not cause significant mass loss, and thermal decomposition is minimal within the material.

On the other hand, electrocatalysts synthesized using the impregnation method exhibit a much more significant thermal degradation pattern. Rapid and substantial mass loss begins at around 400°C, with a total mass loss of approximately 45% at 1000°C. This pattern indicates that the electrocatalysts produced using the impregnation method contain thermally unstable components, such as organic materials or precursors that were not fully converted during the synthesis process. As these components degrade and are lost, a decrease in the active surface area leads to a reduction in electrode conductivity, further compromising performance (Connor *et al.*, 2020).

The impregnation method involves immersing activated carbon powder in a Sn precursor solution, which is then dried and calcined. This process often leaves behind solvent residues and precursors that are not strongly bound to the activated carbon surface. Sn precursors may penetrate deeper into the pores of the activated carbon. The calcination process aims to remove the solvent and convert the precursors into Sn, but it can also cause thermal decomposition of residual organic or inorganic compounds (Y. Li *et al.*, 2018). During TGA, these residues, including those trapped in the pores, evaporate or decompose, resulting in greater and more significant mass loss compared to the precipitation method.

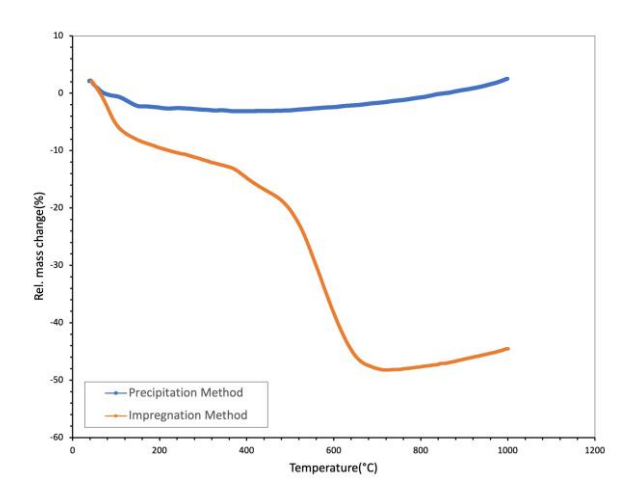


Fig 8. TGA results for the precipitation and impregnation methods.

Based on these results, electrodes synthesized using the precipitation method are more suitable for electrochemical CO_2 reduction applications, especially if the process involves high operating temperatures or repeated thermal cycles. The superior thermal stability of the precipitation method will help maintain the structure and performance of the electrocatalyst during reactions. In contrast, the electrocatalysts from the impregnation method experience significant degradation at high temperatures, which may affect their performance in CO_2 reduction reactions and reduce their lifespan.

3.4. Electrochemical Analysis

3.4.1 CO₂ Reduction Potential of Sn/C Electrode

Electrochemical analysis was conducted to observe the $\rm CO_2$ reduction potential using cyclic voltammetry (CV) on various working electrodes synthesized through precipitation and impregnation methods. The tests were performed using a potentiostat at a scan rate of 50 mV/s over a potential range of 1.5 V to -3 V (vs. SCE).

Fig.9 displays the cyclic voltammograms (CV) of the various Sn/C electrodes with different deposition times, as well as the graphite electrode for comparison. Fig.9(a) shows a comparison of the CV of the graphite electrode under conditions with CO_2 gas and without CO_2 (using N_2 gas as an inert gas). At the same voltage, -2.5 V vs. SCE, the current response observed on the

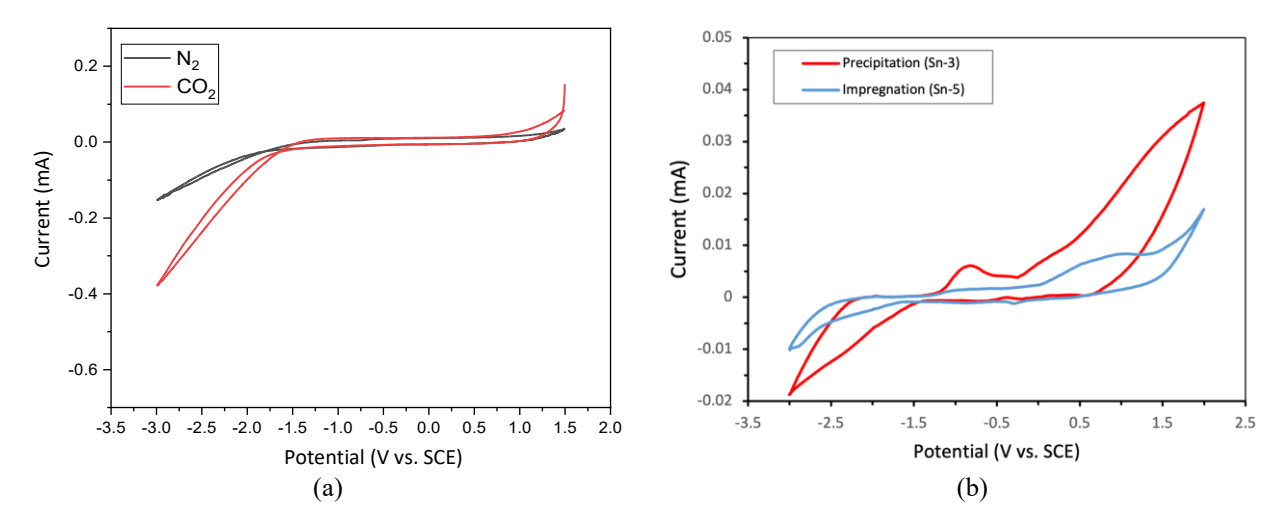


Fig 9. Cyclic voltammograms of electrodes (a) graphite electrode, (b) Sn-3 (precipitation) and Sn-5 (impregnation) electrodes with CO₂

graphite electrode increased to -1.8 mA. A significant increase in current is seen under CO_2 bubbling conditions, particularly in the cathodic region, indicating the occurrence of CO_2 reduction on the graphite electrode surface. In Fig.9(b), a decrease in cathodic current is observed when CO_2 gas is introduced, to -1.5 mA and -0.8 mA for the Sn-3 (precipitation) and Sn-5 (impregnation) electrodes, respectively, compared to the graphite electrode. This shows a reduction in the catalytic activity of the electrodes for reducing CO_2 to products such as formic acid (S. Liu *et al.*, 2019; S. Zhang *et al.*, 2014). The observed low current indicates that additional doping or alternative synthesis methods may be needed to improve performance.

3.4.2 Chronoamperometry

The potential for CO_2 electroreduction testing was determined using data from previous electrochemical analyses. Based on the I-V curve data, equilibrium potential was reached at potentials up to 3.5 V, with ohmic potential observed starting at 3.5 V. In this study, the CO_2 electroreduction experiment was initiated at a potential of 4 V for all Sn/C electrode variations. The current response during the electrolysis process is shown in Fig.10.

The chronoamperometry graph illustrates the current response over time for two Sn/C electrodes prepared by precipitation method (Sn-3) and impregnation method (Sn-5), when subjected to a constant reduction potential of 4 V. Both electrodes exhibit similar overall behavior, characterized by an initial sharp current spike followed by a rapid decay within the first 20 minutes, eventually stabilizing to a steady-state current for the remainder of the 180-minute experiment. The precipitation method (Sn-3) demonstrates marginally superior performance, with both a higher initial current peak (54 mA vs. 48 mA) and a slightly elevated steady-state current (~39-40 mA vs. ~37-38 mA) compared to the impregnation method (Sn-5). This suggests that the precipitation technique may have resulted in a more accessible and/or larger surface area of active Sn sites (C. Wang et al., 2017). The initial current spike likely represents the rapid reduction of easily accessible Sn species on the electrode surface, while the subsequent decay indicates the depletion of these readily available species and a transition to a diffusion-limited process (Anon, 2019; Sandford et al., 2019). The stability of the current over extended periods for both electrodes indicates good overall stability, with the

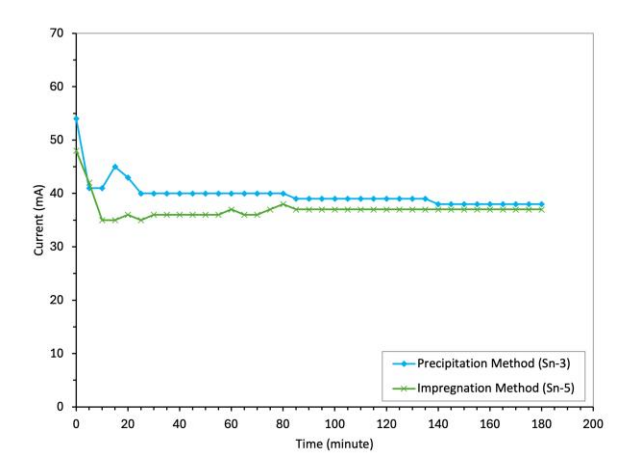


Fig 10. Chronoamperometry graph during electrolysis

precipitation method showing a slight edge in sustained current output. Despite the different preparation methods, the similar curve shapes suggest that the underlying electrochemical processes are likely comparable for both electrodes. The precipitation method appears to yield marginally better electrochemical performance under these specific conditions, potentially offering improved efficiency in applications requiring sustained current output.

3.4.3 Electrochemical Impedance Spectroscopy (EIS)

Electrochemical impedance spectroscopy (EIS) was conducted to evaluate the impedance characteristics of Sn/C electrodes during CO_2 electroreduction. Impedance values were measured in ohms (Ω) , representing the combined bulk resistance and grain boundary resistance. The analysis was performed using an H-type cell, with impedance measured across a frequency range of 100 mHz to 100 kHz. Prior to measurement, the electrolyte was saturated with CO_2 until equilibrium was reached. The Nyquist plots obtained from EIS characterization are shown in Fig.11.

The Nyquist plot was analysed using model fitting, as shown in Fig.12, to determine the values of the Ohmic resistance, as summarized in Table 4. Figure 12 *illustrates* the equivalent circuit model *employed* for Nyquist plot fitting, which serves as

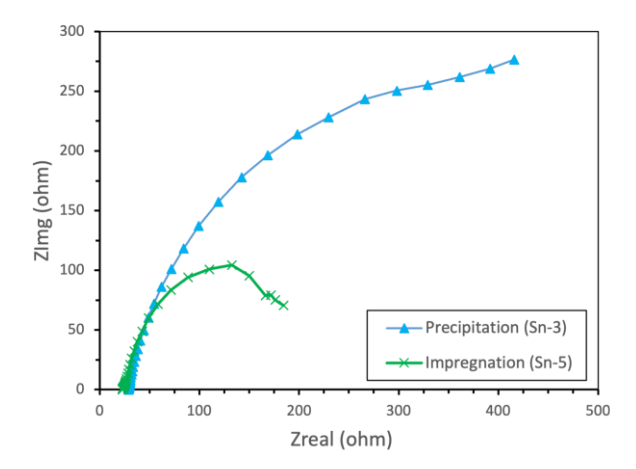


Fig 11. Nyquist plot of Sn/C from precipitation and impregnation method

the theoretical *foundation* for interpreting EIS results. This model is essential for correlating electrode structure with electrochemical performance and validating the comparative evaluation of different synthesis methods by enabling the extraction of critical electrochemical parameters through systematic analysis of impedance data across various frequency ranges.

In the equivalent circuit modeling approach, polarization data from each component can be systematically converted into specific resistance values based on their physical origins and frequency characteristics. The model identifies three primary resistance components that correspond to distinct electrochemical processes: the bulk resistance of the electrolyte (Rb), which is influenced by the electrode-electrolyte interface and corresponds to the intercept of the Nyquist curve with the real impedance axis at high frequency; the grain boundary resistance (Rgb), which represents the ionic transfer resistance observed at medium frequency; and the electrode resistance (Re), which refers to the mass transfer resistance at the electrode-electrolyte interface appearing at low frequency (S. Liu et al., 2019). A critical modification in the equivalent circuit modeling addresses the capacitive behavior, where the porous nature of the electrode necessitates the use of constant phase elements (CPE) rather than ideal capacitors to accurately represent non-ideal capacitive behavior, with CPEgb representing the capacitance at the grain boundary and CPEe representing the electrode capacitance. The total electrolyte resistance (Rt) is determined by summing the bulk resistance (Rb) and the grain boundary resistance (Rgb), providing a comprehensive quantitative assessment of the overall electrochemical impedance characteristics (Bisquert et al., 2000; Hernández et al., 2016; McNealy and Hertz, 2014).

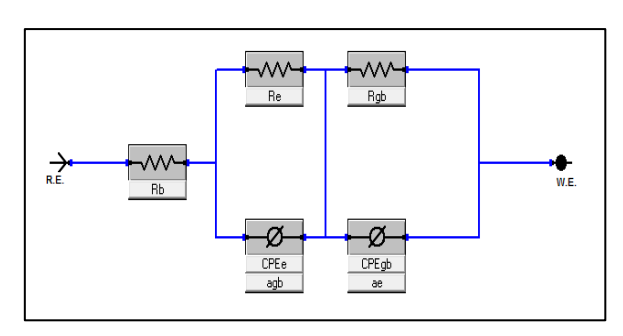


Fig 12. Nyquist Fitting

Table 4 Fitting results of Sn/C electrodes

R _{ohmic} (ohm)	
38,1	
28,8	
29,8	

The precipitation method (Sn-3) sample shows a larger overall impedance (wider semicircle), which suggests higher values for Re, Rgb, or both, compared to the Impregnation (Sn-5) sample. This indicates that the precipitation method may result in higher interfacial and/or grain boundary resistances, despite its slightly lower ohmic resistance (Lazanas & Prodromidis, 2023; Pía Canales, 2022) The Impregnation (Sn-5) sample, with its smaller semicircle, likely has lower Re and Rgb values, indicating better charge transfer characteristics and potentially better integration of the active material within the electrode structure (Laschuk et al., 2021; Padha et al., 2022) This could be due to a more uniform distribution of the Sn within the electrode achieved by the impregnation method (T. Zhao et al., 2011). The use of CPEs instead of ideal capacitors suggests that both samples have some degree of surface roughness or inhomogeneity, which is common in real electrochemical systems (Jorcin et al., 2006). The specific values of these CPEs would provide insights into the capacitive behavior and the nature of the electrode-electrolyte interfaces.

While the Precipitation method yields a marginally lower ohmic resistance, the overall electrochemical performance appears to be superior in the Impregnation sample. This is evidenced by the lower total impedance and suggests that the impregnation method may result in a more favorable electrode structure for charge transfer and ion movement. These findings highlight the importance of considering not just the bulk resistance, but also the interfacial and charge transfer processes when optimizing electrode preparation methods for electrochemical applications. These results indicate that Sn exhibits a high conductivity on the graphite electrode, thereby reducing the ohmic resistance, which in turn accelerates electron transfer (Savino et al., 2022; Dang et al., 2024).

4. Conclusion

The comprehensive analysis of Sn/C electrodes synthesized through precipitation and impregnation methods for ECO₂R to formic acid reveals a complex interplay of factors affecting electrode performance. Although both methods provide unique benefits, the precipitation-synthesized electrode is preferred for CO₂ electrolysis to produce formic acid. This suggestion is predicated on several critical factors, including its exceptionally high Sn content (91.22%), excellent thermal stability with only 3% mass loss at 1000°C, and marginally enhanced sustained performance in chronoamperometry tests. Despite the enhanced charge transfer characteristics of impregnationsynthesized electrodes, the precipitation method improved tin content and thermal stability render it more advantageous for long-term, industrial-scale applications. However, it is crucial to acknowledge that neither electrode surpassed pure graphite regarding catalytic activity for CO2 reduction, highlighting the necessity for additional optimization. Future study should concentrate on improving the catalytic activity of precipitationsynthesized Sn/C electrodes while maintaining their high Sn concentration and thermal stability. Strategies could involve optimizing the precipitation process, examining hybrid synthesis methods, or researching dopants to enhance charge

transfer while maintaining stability. The study underscores the significance of comprehensive characterization in electrode development, as the inconsistency between elevated Sn concentration and decreased catalytic activity indicates complex surface interactions that necessitate additional examination. In conclusion, although the precipitation-synthesized Sn/C electrode is suggested for CO_2 electrolysis to produce formic acid due to its favorable characteristics, substantial enhancements are necessary. Further studies should focus on reconciling the high Sn content with the necessary catalytic activity, potentially resulting in more efficient and economically feasible ECO_2R processes for formic acid production.

Acknowledgements.

We acknowledge the support of Badan Pengelola Dana Perkebunan Kelapa Sawit (BPDPKS) under the grant Number PRJ-133/DPKS/2024.

References

- Ali, A. M., Zahrani, A. A., Daous, M. A., Podila, S., Alshehri, M. K., Rather, S., & Saeed, U. (2022). Sequential and/or Simultaneous Wet-Impregnation Impact on the Mesoporous Pt/Sn/Zn/γ -Al₂O₃ Catalysts for the Direct Ethane Dehydrogenation. *Journal of Nanomaterials*, 2022(1). https://doi.org/10.1155/2022/8739993
- Álvarez-Gómez, J. M., & Varela, A. S. (2023). Review on Long-Term Stability of Electrochemical CO₂ Reduction. *Energy & Fuels*, *37*(20), 15283–15308. https://doi.org/10.1021/acs.energyfuels.3c01847
- Anon. (2019). Voltammetric Methods https://chem.libretexts.org/@go/page/70712
- Bashir, S., Hossain, Sk. S., Rahman, S. ur, Ahmed, S., Amir Al-Ahmed, & Hossain, M. M. (2016). Electrocatalytic reduction of carbon dioxide on SnO₂/MWCNT in aqueous electrolyte solution. *Journal of CO₂ Utilization*, 16, 346–353. https://doi.org/10.1016/j.jcou.2016.09.002
- Bisquert, J., Garcia-Belmonte, G., Fabregat-Santiago, F., Ferriols, N. S., Bogdanoff, P., & Pereira, E. C. (2000). Doubling Exponent Models for the Analysis of Porous Film Electrodes by Impedance. Relaxation of TiO_2 Nanoporous in Aqueous Solution. *The Journal of Physical Chemistry B*, 104(10), 2287–2298. https://doi.org/10.1021/jp993148h
- Botchway, E. A., Ampong, F. K., Nkrumah, I., Puzer, D. B., Nkum, R. K., & Boakye, F. (2023). The CZTS Thin Films Grown by Sulfurization of Electrodeposited Metallic Precursors: The Effect of Increasing Tin Content of the Metallic Precursors on the Structure, Morphology and Optical Properties of the Thin Films. East European Journal of Physics, 2, 249–256. https://doi.org/10.26565/2312-4334-2023-2-28
- Connor, P., Schuch, J., Kaiser, B., & Jaegermann, W. (2020). The Determination of Electrochemical Active Surface Area and Specific Capacity Revisited for the System MnO_x as an Oxygen Evolution Catalyst. Zeitschrift Für Physikalische Chemie, 234(5), 979–994. https://doi.org/10.1515/zpch-2019-1514
- Dang, H., Guan, B., Chen, J., Ma, Z., Chen, Y., Zhang, J., Guo, Z., Chen, L., Hu, J., Yi, C., Yao, S., & Huang, Z. (2024). Research Status, Challenges, and Future Prospects of Carbon Dioxide Reduction Technology. *Energy & Fuels*, 38(6), 4836–4880. https://doi.org/10.1021/acs.energyfuels.3c04591
- Del Castillo, A., Alvarez-Guerra, M., & Irabien, A. (2014). Continuous electroreduction of CO_2 to formate using Sn gas diffusion electrodes. *AIChE Journal*, 60(10), 3557–3564. https://doi.org/10.1002/aic.14544
- del Castillo, A., Alvarez-Guerra, M., Solla-Gullón, J., Sáez, A., Montiel, V., & Irabien, A. (2015). Electrocatalytic reduction of CO₂ to formate using particulate Sn electrodes: Effect of metal loading and particle size. Applied Energy, 157, 165–173. https://doi.org/10.1016/j.apenergy.2015.08.012
- Del Castillo, A., Alvarez-Guerra, M., Solla-Gullón, J., Sáez, A., Montiel, V., & Irabien, A. (2017). Sn nanoparticles on gas diffusion

- electrodes: Synthesis, characterization and use for continuous CO₂ electroreduction to formate. *Journal of CO2 Utilization*, *18*, 222–228. https://doi.org/10.1016/j.jcou.2017.01.021
- Dinh, C.-T., García de Arquer, F. P., Sinton, D., & Sargent, E. H. (2018). High Rate, Selective, and Stable Electroreduction of CO₂ to CO in Basic and Neutral Media. *ACS Energy Letters*, 3(11), 2835–2840. https://doi.org/10.1021/acsenergylett.8b01734
- Hernández, M. A., Masó, N., & West, A. R. (2016). On the correct choice of equivalent circuit for fitting bulk impedance data of ionic/electronic conductors. *Applied Physics Letters*, *108*(15). https://doi.org/10.1063/1.4946008
- IEA. (2024). CO2 Emissions in 2023. https://www.iea.org/reports/co2emissions-in-2023
- Jorcin, J.-B., Orazem, M. E., Pébère, N., & Tribollet, B. (2006). CPE analysis by local electrochemical impedance spectroscopy. *Electrochimica Acta*, 51(8–9), 1473–1479. https://doi.org/10.1016/j.electacta.2005.02.128
- Kim, H.-Y., Choi, I., Ahn, S. H., Hwang, S. J., Yoo, S. J., Han, J., Kim, J., Park, H., Jang, J. H., & Kim, S.-K. (2014). Analysis on the effect of operating conditions on electrochemical conversion of carbon dioxide to formic acid. *International Journal of Hydrogen Energy*, 39(29), 16506–16512. https://doi.org/10.1016/j.ijhydene.2014.03.145
- Laschuk, N. O., Easton, E. B., & Zenkina, O. V. (2021). Reducing the resistance for the use of electrochemical impedance spectroscopy analysis in materials chemistry. RSC Advances, 11(45), 27925–27936. https://doi.org/10.1039/D1RA03785D
- Lazanas, A. Ch., & Prodromidis, M. I. (2023). Electrochemical Impedance Spectroscopy—A Tutorial. *ACS Measurement Science Au*, *3*(3), 162–193. https://doi.org/10.1021/acsmeasuresciau.2c00070
- Li, Q., Wang, Z., Zhang, M., Hou, P., & Kang, P. (2017). Nitrogen doped tin oxide nanostructured catalysts for selective electrochemical reduction of carbon dioxide to formate. *Journal of Energy Chemistry*, 26(5), 825–829. https://doi.org/10.1016/j.jechem.2017.08.010
- Li, W., Liu, J., & Yan, C. (2011). Electrochimica Acta Graphite graphite oxide composite electrode for vanadium redox flow battery. *Electrochimica Acta*, 56(14), 5290–5294. https://doi.org/10.1016/j.electacta.2011.02.083
- Li, W., Seredych, M., Rodríguez-Castellón, E., & Bandosz, T. J. (2016). Metal-free Nanoporous Carbon as a Catalyst for Electrochemical Reduction of CO₂ to CO and CH 4. *ChemSusChem*, 9(6), 606–616. https://doi.org/10.1002/cssc.201501575
- Li, Y., Han, X., Fu, S., Guo, L., Chen, S., & Wang, J. (2025). Hydrophobic modification of hydroxyl-rich metallic Sn catalysts for acidic CO₂ electroreduction at high current densities. *Catalysis Science & Technology*. https://doi.org/10.1039/D5CY00424A
- Li, Y., Yang, Q., Wang, Z., Wang, G., Zhang, B., Zhang, Q., & Yang, D. (2018). Rapid fabrication of SnO₂ nanoparticle photocatalyst: computational understanding and photocatalytic degradation of organic dye. *Inorganic Chemistry Frontiers*, *5*(12), 3005–3014. https://doi.org/10.1039/C8QI00688A
- Lim, J. W., Dong, W. J., Park, J. Y., Hong, D. M., & Lee, J.-L. (2020). Spontaneously Formed CuS_x Catalysts for Selective and Stable Electrochemical Reduction of Industrial CO₂ Gas to Formate. *ACS Applied Materials & Interfaces*, 12(20), 22891–22900. https://doi.org/10.1021/acsami.0c03606
- Liu, H., Shi, E., Guo, W., Sun, Z., Fang, Z., Zhu, Z., Jiao, L., Zhai, Y., & Lu, X. (2023). Selectivity control for CO_2 electroreduction to syngas using Fe/CuO_x catalysts with high current density. *Chemical Communications*, 59(64), 9746–9749. https://doi.org/10.1039/D3CC03328G
- Liu, S., Yang, H., Su, X., Ding, J., Mao, Q., Huang, Y., Zhang, T., & Liu, B. (2019). Rational design of carbon-based metal-free catalysts for electrochemical carbon dioxide reduction: A review. *Journal of Energy Chemistry*, 36, 95–105. https://doi.org/10.1016/j.jechem.2019.06.013
- Maximize Market Research. (2024). Formic Acid Market: Global Application Analysis and Forecast (2025-2032) Trends, Statistics, Dynamics, Segmentation by Grade Type, Price Point, Distribution Channel, and Region. https://www.maximizemarketresearch.com/marketreport/formic-acid-market/190968/
- McNealy, B. E., & Hertz, J. L. (2014). On the Utility of Constant Phase Elements to Characterize Heterogeneous Ceramic Grain

- Boundaries. ECS Meeting Abstracts, MA2014-01(16), 756-756. https://doi.org/10.1149/MA2014-01/16/756
- Miki, Y., Takeuchi, W., Nakatsuka, O., & Zaima, S. (2019). Influence of Sn precursors on Ge_{1-x} Sn_x growth using metal-organic chemical vapor deposition. *Japanese Journal of Applied Physics*, 58(SA), SAAD07. https://doi.org/10.7567/1347-4065/aaec1a
- Monteiro, M. C. O., Dattila, F., López, N., & Koper, M. T. M. (2022). The Role of Cation Acidity on the Competition between Hydrogen Evolution and CO₂ Reduction on Gold Electrodes. *Journal of the American Chemical Society*, 144(4), 1589–1602. https://doi.org/10.1021/jacs.1c10171
- Nkrumah, I., Ampong, F. K., Britwum, A., Paal, M., Kwakye-Awuah, B., Nkum, R. K., & Boakye, F. (2023). The effect of the concentration of tin (Sn) in the metallic precursor, on the structure, morphology, optical and electrical properties of electrochemically deposited lead-tin-sulphide (PbSnS) thin films. *Chalcogenide Letters*, 20(6), 399–407. https://doi.org/10.15251/CL.2023.206.399
- Padha, B., Verma, S., Mahajan, P., & Arya, S. (2022). Electrochemical Impedance Spectroscopy (EIS) Performance Analysis and Challenges in Fuel Cell Applications. *Journal of Electrochemical Science and Technology*, 13(2), 167–176. https://doi.org/10.33961/jecst.2021.01263
- Pía Canales, C. (2022). Electrochemical Impedance Spectroscopy and Its Applications. In 21st Century Nanostructured Materials Physics, Chemistry, Classification, and Emerging Applications in Industry, Biomedicine, and Agriculture. IntechOpen. https://doi.org/10.5772/intechopen.101636
- Qu, G., Wei, K., Pan, K., Qin, J., Lv, J., Li, J., & Ning, P. (2023). Emerging materials for electrochemical CO₂ reduction: progress and optimization strategies of carbon-based single-atom catalysts. *Nanoscale*, 15(8), 3666–3692. https://doi.org/10.1039/D2NR06190B
- Ren, M., Zheng, H., Lei, J., Zhang, J., Wang, X., Yakobson, B. I., Yao, Y., & Tour, J. M. (2020). CO₂ to Formic Acid Using Cu–Sn on Laser-Induced Graphene. ACS Applied Materials & Interfaces, 12(37), 41223–41229. https://doi.org/10.1021/acsami.0c08964
- Safaei, J., Mohamed, N. A., Mohamad Noh, M. F., Soh, M. F., Ludin, N. A., Ibrahim, M. A., Roslam Wan Isahak, W. N., & Mat Teridi, M. A. (2018). Graphitic carbon nitride (g-C₃N₄) electrodes for energy conversion and storage: a review on photoelectrochemical water splitting, solar cells and supercapacitors. *Journal of Materials Chemistry* A, 6(45), 22346–22380. https://doi.org/10.1039/C8TA08001A
- Sandford, C., Edwards, M. A., Klunder, K. J., Hickey, D. P., Li, M., Barman, K., Sigman, M. S., White, H. S., & Minteer, S. D. (2019). A synthetic chemist's guide to electroanalytical tools for studying reaction mechanisms. *Chemical Science*, 10(26), 6404–6422. https://doi.org/10.1039/C9SC01545K
- Satola, B., Kirchner, C. N., Komsiyska, L., & Wittstock, G. (2016). Chemical Stability of Graphite-Polypropylene Bipolar Plates for the Vanadium Redox Flow Battery at Resting State. *Journal of The Electrochemical Society*, 163(10), A2318–A2325. https://doi.org/10.1149/2.0841610jes
- Savino, U., Sacco, A., Bejtka, K., Castellino, M., Farkhondehfal, M. A., Chiodoni, A., Pirri, F., & Tresso, E. (2022). Well performing Fe-SnO₂ for CO₂ reduction to HCOOH. 163. https://doi.org/10.1016/j.catcom.2022.106412
- Shaikh, N. S., Shaikh, J. S., Márquez, V., Pathan, S. C., Mali, S. S., Patil, J. V., Hong, C. K., Kanjanaboos, P., Fontaine, O., Tiwari, A., Praserthdam, S., & Praserthdam, P. (2023). New perspectives, rational designs, and engineering of Tin (Sn)-based materials for electrochemical CO₂ reduction. *Materials Today Sustainability*, 22, 100384. https://doi.org/10.1016/j.mtsust.2023.100384
- $\label{eq:Varhade, S., Guruji, A., Singh, C., Cicero, G., García-Melchor, M., Helsen, J., & Pant, D. (2025). Electrochemical CO_2 Reduction: Commercial Innovations and Prospects. {\it ChemElectroChem}, 12(2). \\ https://doi.org/10.1002/celc.202400512$
- Wang, C., Chen, Y., Jiang, J., Zhang, R., Niu, Y., Zhou, T., Xia, J., Tian, H., Hu, J., & Yang, P. (2017). Improved thermoelectric properties of SnS synthesized by chemical precipitation. RSC Advances, 7(27), 16795–16800. https://doi.org/10.1039/C7RA00373K
- Wang, J., Ji, Y., Shao, Q., Yin, R., Guo, J., Li, Y., & Huang, X. (2019). Phase and structure modulating of bimetallic CuSn nanowires boosts electrocatalytic conversion of CO₂. *Nano Energy*, *59*, 138–145. https://doi.org/10.1016/j.nanoen.2019.02.037

- Wang, Q., Wang, X., Wu, C., Cheng, Y., Sun, Q., Dong, H., & Yu, H. (2017). Electrodeposition of tin on Nafion-bonded carbon black as an active catalyst layer for efficient electroreduction of CO₂ to formic acid. *Scientific Reports*, 7(1), 13711. https://doi.org/10.1038/s41598-017-14233-y
- Wen, G., Lee, D. U., Ren, B., Hassan, F. M., Jiang, G., Cano, Z. P., Gostick, J., Croiset, E., Bai, Z., Yang, L., & Chen, Z. (2018). Orbital Interactions in Bi-Sn Bimetallic Electrocatalysts for Highly Selective Electrochemical CO₂ Reduction toward Formate Production. Advanced Energy Materials, 8(31), 1802427. https://doi.org/10.1002/aenm.201802427
- Widiatmoko, P., Nurdin, I., Devianto, H., Prakarsa, B., & Hudoyo, H. (2020). Electrochemical reduction of CO₂ to Formic Acid on Pb-Sn Alloy Cathode. *IOP Conference Series: Materials Science and Engineering*, 823(1), 012053. https://doi.org/10.1088/1757-899X/823/1/012053
- Won, D. H., Choi, C. H., Chung, J., Chung, M. W., Kim, E.-H., & Woo, S. I. (2015). Rational Design of a Hierarchical Tin Dendrite Electrode for Efficient Electrochemical Reduction of CO₂. *ChemSusChem*, 8(18), 3092–3098. https://doi.org/10.1002/cssc.201500694
- Wu, Z., Wu, H., Cai, W., Wen, Z., Jia, B., Wang, L., Jin, W., & Ma, T. (2021). Engineering Bismuth–Tin Interface in Bimetallic Aerogel with a 3D Porous Structure for Highly Selective Electrocatalytic CO₂ Reduction to HCOOH. *Angewandte Chemie International Edition*, 60(22), 12554–12559. https://doi.org/10.1002/anie.202102832
- Yang, Q., Wu, Q., Liu, Y., Luo, S., Wu, X., Zhao, X., Zou, H., Long, B., Chen, W., Liao, Y., Li, L., Shen, P. K., Duan, L., & Quan, Z. (2020).
 Novel Bi-Doped Amorphous SnO x Nanoshells for Efficient Electrochemical CO2 Reduction into Formate at Low Overpotentials. Advanced Materials, 2002822. https://doi.org/10.1002/adma.202002822
- Yao, Y., Zhuang, W., Li, R., Dong, K., Luo, Y., He, X., Sun, S., Alfaifi, S., Sun, X., & Hu, W. (Walter). (2023). Sn-based electrocatalysts for electrochemical CO₂ reduction. *Chemical Communications*, 59(59), 9017–9028. https://doi.org/10.1039/D3CC02531D
- Yu, H., Wu, L., Ni, B., & Chen, T. (2023). Research Progress on Porous Carbon-Based Non-Precious Metal Electrocatalysts. *Materials* (Vol. 16 (8).. https://doi.org/10.3390/ma16083283
- Zhang, H., Min, S., Wang, F., Zhang, Z., & Kong, C. (2020). Efficient electrocatalytic CO₂ reduction to CO with high selectivity using a N-doped carbonized wood membrane. *New Journal of Chemistry*, 44(16), 6125–6129. https://doi.org/10.1039/D0NJ00538J
- Zhang, K., Zhang, H., Ma, H., Ying, W., & Fang, D. (2015). The effect of preparation method on the performance of PtSn/Al₂O₃ catalysts for acetic acid hydrogenation. *Polish Journal of Chemical Technology*, 17(1), 11–17. https://doi.org/10.1515/pjct-2015-0003
- Zhang, R., Lv, W., Li, G., & Lei, L. (2015). Electrochemical reduction of CO₂ on SnO₂/nitrogen-doped multiwalled carbon nanotubes composites in KHCO₃ aqueous solution. *Materials Letters*, *141*, 63–66. https://doi.org/10.1016/j.matlet.2014.11.040
- Zhang, R., Lv, W., Li, G., Mezaal, M. A., & Lei, L. (2015). Electrochemical reduction of carbon dioxide to formate with a Sn cathode and an Ir_xSn_yRu_zO₂/Ti anode. *RSC Advances*, *5*(84), 68662–68667. https://doi.org/10.1039/C5RA13618K
- Zhang, S., Kang, P., & Meyer, T. J. (2014). Nanostructured Tin Catalysts for Selective Electrochemical Reduction of Carbon Dioxide to Formate. *Journal of the American Chemical Society*, 136(5), 1734–1737. https://doi.org/10.1021/ja4113885
- Zhao, C., Wang, J., & Goodenough, J. B. (2016). Comparison of electrocatalytic reduction of CO₂ to HCOOH with different tin oxides on carbon nanotubes. *Electrochemistry Communications*, *65*, 9–13. https://doi.org/10.1016/j.elecom.2016.01.019
- Zhao, S., Li, S., Guo, T., Zhang, S., Wang, J., Wu, Y., & Chen, Y. (2019).

 Advances in Sn-Based Catalysts for Electrochemical CO₂
 Reduction. *Nano-Micro Letters*, 11(1), 62.

 https://doi.org/10.1007/s40820-019-0293-x
- Zhao, T., Boullosa-Eiras, S., Yu, Y., Chen, D., Holmen, A., & Ronning, M. (2011). Synthesis of Supported Catalysts by Impregnation and Calcination of Low-Temperature Polymerizable Metal-Complexes. Topics in Catalysis, 54(16–18), 1163–1174. https://doi.org/10.1007/s11244-011-9738-2
- Zhu, C., Yu, A., Zhang, Y., Chen, W., Wu, Z., Xu, M., Qu, D., Duan, J., & Li, X. (2025). Cu-Sn Electrocatalyst Prepared with Chemical Foaming and Electroreduction for Electrochemical CO₂ Reduction. *Catalysts*, *15*(5), 484. https://doi.org/10.3390/catal15050484

Zhu, Q., Ma, J., Kang, X., Sun, X., Liu, H., Hu, J., Liu, Z., & Han, B. (2016). Efficient Reduction of CO2 into Formic Acid on a Lead or Tin Electrode using an Ionic Liquid Catholyte Mixture. Angewandte

9012-9016. ChemieEdition, *55*(31), International https://doi.org/10.1002/anie.201601974



© 2025. The Author(s). This article is an open access article distributed under the terms and conditions of the Creative Commons Attribution-ShareAlike 4.0 (CC BY-SA) International License (http://creativecommons.org/licenses/by-sa/4.0/)